Epilepsia, 52(12):2267–2275, 2011
doi: 10.1111/j.1528-1167.2011.03313.x

FULL-LENGTH ORIGINAL RESEARCH

Distinct white matter abnormalities in different idiopathic generalized epilepsy syndromes

***Min Liu, †Luis Concha, *Christian Beaulieu, and ‡Donald W. Gross**

***Department of Biomedical Engineering, Faculty of Medicine and Dentistry, University of Alberta, Edmonton, Alberta, Canada; †Institute of Neurobiology, National Autonomous University of México, Queretaro, Mexico; and ‡Division of Neurology, Department of Medicine, Faculty of Medicine and Dentistry, University of Alberta, Edmonton, Alberta, Canada**

Summary

Purpose: By definition idiopathic generalized epilepsy (IGE) is not associated with structural abnormalities on conventional magnetic resonance imaging (MRI). However, recent quantitative studies suggest white and gray matter alterations in IGE. The purpose of this study was to investigate whether there are white and/or gray matter structural differences between controls and two subsets of IGE, namely juvenile myoclonic epilepsy (JME) and IGE with generalized tonic–clonic seizures only (IGE-GTC).

Methods: We assessed white matter integrity and gray matter volume using diffusion tensor tractography–based analysis of fractional anisotropy and voxel-based morphometry, respectively, in 25 patients with IGE, all of whom had experienced generalized tonic–clonic convulsions. Specifically, 15 patients with JME and 10 patients with IGE-GTC were compared to two groups of similarly matched controls separately. Correlations between total lifetime generalized tonic–clonic seizures and fractional anisotropy were investigated for both groups.

Key Findings: Tractography revealed lower fractional anisotropy in specific tracts including the crus of the fornix, body of corpus callosum, uncinate fasciculi, superior longitudinal fasciculi, anterior limb of internal capsule, and corticospinal tracts in JME with respect to controls, whereas there were no fractional anisotropy differences in IGE-GTC. No correlation was found between fractional anisotropy and total lifetime generalized tonic–clonic seizures for either JME or IGE-GTC. Although false discovery rate–corrected voxel-based morphometry (VBM) showed no gray matter volume differences between patient and control groups, spatial extent cluster–corrected VBM analysis suggested a trend of gray matter volume reduction in frontal and central regions in both patient groups, more lateral in JME and more medial in IGE-GTC.

Significance: The findings support the idea that the clinical syndromes of JME and IGE-GTC have unique anatomic substrates. The fact that the primary clinical difference between JME and IGE-GTC is the occurrence of myoclonus in the former raises the possibility that disruption of white matter integrity may be the underlying mechanism responsible for myoclonus in JME. The cross-sectional study design and relatively small number of subjects limits the conclusions that can be drawn here; however, the absence of a correlation between fractional anisotropy and lifetime seizures is suggestive that the white matter abnormalities observed in JME may not be secondary to seizures.

KEY WORDS: Idiopathic generalized epilepsy, Juvenile myoclonic epilepsy, Tractography, Diffusion tensor imaging.

The underlying cause of idiopathic generalized epilepsy (IGE) remains unknown. By definition IGE is not associated with structural abnormalities on conventional magnetic resonance imaging (MRI) (ILAE 1989). This, together with recent genetic studies demonstrating ion channel and neurotransmitter receptor defects in a small number of pedigrees with autosomal dominant inherited juvenile myoclonic epilepsy (JME) (Cossette et al., 2002), has led to the notion that the underlying pathophysiologic mechanisms responsible for sporadic IGE occur at the molecular/membrane level. IGE is subdivided into different syndromes based on the predominant seizure type and age of onset (ILAE 1989; Engel, 2001). JME, the most common IGE subsyndrome, is associated with the occurrence of ''impulsive petit mal'' or myoclonus, which is the primary clinical feature that distinguishes it from IGE with generalized tonic–clonic convulsions only (IGE-GTC) (Janz, 1985; Engel, 2001; Camfield & Camfield, 2010). Recent genetic studies suggest that JME should be considered separately from other subtypes of IGE based on its distinct genetic bases (Zifkin et al., 2005). On the other hand, the overlapping clinical phenotypes and lack

Accepted September 20, 2011; Early View publication November 16, 2011.
Address correspondence to Dr. Donald W. Gross, Division of Neurology, Department of Medicine, 2E3.19 Walter C Mackenzie Health Sciences Centre, Edmonton, AB T6G 2B7, Canada. E-mail: donald.gross@ualberta.ca

of specificity of electroencephalography (EEG) manifestations makes the differentiation between the two syndromes difficult (Janz, 1985; Andermann & Berkovic, 2001; Koutroumanidis & Smith, 2005).

Recent advances in quantitative neuroimaging enable detailed investigation of the brain in vivo. A few studies in single voxel magnetic resonance spectroscopy (MRS) or magnetic resonance spectroscopic imaging (MRSI) have provided evidence of both cortical and deep gray matter (GM) abnormalities, particularly in frontal lobe and thalamus, in IGE patients (Savic et al., 2000; Bernasconi et al., 2003; Mory et al., 2003; Savic et al., 2004; Helms et al., 2006; Haki et al., 2007; Lin et al., 2009; Doelken et al., 2010). However, findings in IGE using MRI volumetry and voxel-based morphometry (VBM) methods on T_1-weighted images have been inconsistent. The first quantitative MRI study on IGE reported significantly larger cortical GM volumes (GMVs) in 45 syndrome-mixed IGE patients compared to controls using a semiautomatic segmentation method (Woermann et al., 1998). More recently, a VBM study of 22 syndrome-mixed IGE patients reported 17 of them with increased cortical GMV and 7 patients with either enlargement or atrophy of thalamus (Betting et al., 2010). Two volumetry studies of the thalami in mixed IGE patients did not detect differences (Natsume et al., 2003; Seeck et al., 2005). In studies investigating JME independently, some reported increased cortical GM in mesial frontal lobes (Woermann et al., 1999; Kim et al., 2007a) or the frontobasal region (Betting et al., 2006a). Other studies suggest decreased GM concentration in the prefrontal lobe (Tae et al., 2006) and thinner cortical thickness of frontal and temporal gyri (Tae et al., 2008). A more recent study reported decreased GM volume in the supplementary motor area and posterior cingulate cortex in JME (O'Muircheartaigh et al., 2011). On the other hand, a recent VBM study failed to demonstrate significant GM differences between JME and age-, sex-, and education-matched controls (Roebling et al., 2009). Bilateral thalamic atrophy was detected in only one VBM study of JME (Kim et al., 2007a) but not in the other groups (Woermann et al., 1999; Betting et al., 2006b; Tae et al., 2006). Some studies also explored underlying GM abnormalities in IGE with generalized tonic–clonic seizures as the predominant seizure type with inconclusive results. One MRI volumetry and VBM study of IGE-GTC revealed reduced cortical GM in the frontal, parietal, and temporal cortices and cerebellum and reduced subcortical GM in the thalamus, caudate, and putamen (Ciumas & Savic, 2006), whereas another study showed widespread cortical thinning in the frontocentral areas and bilateral thalamic atrophy (Bernhardt et al., 2009). A more recent study on IGE-GTC reported atrophy in the left thalamus, left putamen, and bilateral globus pallidus (Du et al., 2011). However, a VBM study showed no GM abnormality in the patients with generalized tonic–clonic seizures on awakening (Betting et al., 2006a). Overall, the most consistent structural findings have been frontocentral alterations in JME with less consistent findings in IGE-GTC patients.

In contrast to the numerous studies with a focus on GM, there is a paucity of research on the white matter (WM) in IGE. Diffusion tensor imaging (DTI) is a technique that measures the diffusion and directionality of water (Basser et al., 1994), which is in turn an indirect marker of key microstructural components of the WM tracts such as axon packing, myelination, and cumulative membrane circumference (Beaulieu, 2002; Concha et al., 2010). Although there have been numerous DTI studies highlighting extensive WM abnormalities in temporal lobe epilepsy (Arfanakis et al., 2002; Concha et al., 2005a; Thivard et al., 2005; Ahmadi et al., 2009; Concha et al., 2009; Yogarajah et al., 2009), it is unknown if similar findings will be observed in IGE. There are four previous DTI studies of JME patients: (1) voxel-based analysis (VBA) identified bilateral fractional anisotropy (FA) reduction in the anterior limb of the internal capsule that correlated with the frequency of generalized tonic–clonic seizures (Deppe et al., 2008); (2) region-of-interest (ROI) analysis showed reduced FA in frontal lobe and thalamocortical WM fibers and increased FA in bilateral putamen in the same group of JME patients studied in (1) (Keller et al., 2011); (3) probabilistic tractography identified an FA reduction and mean diffusivity (MD) elevation of the callosal tracts bridging the left and right supplementary motor areas and left corticospinal tracts, and a small number of fibers connecting to the primary motor cortex (Vulliemoz et al., 2011); and (4) tract-based spatial statistics (TBSS) showed reduced FA in the rostral body and splenium of the corpus callosum (O'Muircheartaigh et al., 2011). There is only one DTI study on IGE-GTC showing decreased FA in cerebellum confirmed by VBA, TBSS, probabilistic tractography, and ROI analyses (Li et al., 2011).

The purpose of this study was to investigate whether there are white and/or gray matter structural differences between controls and two subsets of IGE, namely JME, and IGE-GTC. White matter microstructure as indicated by FA was analyzed using diffusion tensor tractography and ROI analysis of 13 major white matter tracts. Regional gray matter volume was assessed using whole-brain VBM of three-dimensional (3D) T_1-weighted images. Correlations of FA with lifetime seizures were measured in both IGE groups.

Subjects and Methods

Approval of the research protocol was obtained from the University of Alberta Health Research Ethics Board, and informed consent was obtained from all participants.

Subjects

Participants included 15 patients with JME (12 female/3 male, age 21 ± 4 years, range 17–32 years) and 10 patients with IGE-GTC (3 female/7 male, age

21 ± 4 years, range 18–31 years) who were recruited from the epilepsy clinic of the University of Alberta Hospital. All patients had a history of GTC seizures, normal intelligence, normal neurologic examination, absence of focal EEG abnormalities, and normal clinical MRI scans. Among the 15 JME patients, 4 were on two AEDs and all the others were on a single medication. Among the 10 IGE-GTC patients, 3 were on two AEDs and all the others were on one medication. Precise total lifetime GTC seizure number was available for 23 of 25 patients. For the remaining 2 patients who had 12–16 and 12–14 seizures, mean values of 14 and 13 were chosen for the correlation analysis. There was no difference in the number of lifetime GTC seizures between the two patient groups (for JME, 6 ± 4 lifetime GTC, range 1–14; for IGE-GTC, 6 ± 4 lifetime GTC, range 1–12; Student's *t*-test, p = 0.98). The 15 JME patients were compared to a group of 15 age-matched controls (12 female/3 male, age 21 ± 4 years, range 17–31 years). The 10 IGE-GTC patients were compared to another group of 10 age-matched controls (3 female/7 male, age 21 ± 4 years, range 18–30 years) distinct from the 15 controls paired with JME patients. All 25 control subjects had no history of any neurologic or psychiatric disorders.

Image acquisition

All imaging was performed on a 1.5T Siemens Sonata scanner (Erlangen, Germany). Three imaging protocols were used, including magnetization prepared rapid acquisition gradient echo (MPRAGE), standard DTI, and fluid-attenuated inversion recovery (FLAIR) DTI. MPRAGE provides high resolution 3D T_1-weighted images that were acquired with the following parameters: 1 mm slice thickness with no interslice gap, 144 axial slices, repetition time (TR) = 1,890 ms, echo time (TE) = 4.38 ms, inversion time (TI) = 1,100 ms, flip angle = 15 degrees, number of excitations (NEX) = 1, acquisition matrix = 256 × 192 (interpolated to 512 × 384), field of view (FOV) = 256 mm × 192 mm, voxel dimension 1 × 1 × 1 mm^3 (interpolated to 0.5 × 0.5 × 1 mm^3), scan time = 6:03 min. The two DTI protocols used the same dual spin-echo, single shot echo planar imaging (EPI) sequence except an extra inversion pulse and fewer slices for FLAIR DTI. The common parameters are: 2 mm thick axial oblique slices with no interslice gap; TR = 10 s, TE = 88 ms, acquisition matrix = 128 × 128 with 75% phase partial Fourier (interpolated to 256 × 256), FOV = 256 mm × 256 mm, voxel dimension 2 × 2 × 2 mm^3 (interpolated to 1 × 1 × 2 mm^3), six diffusion directions, b = 1,000 s/mm^2, eight averages. The protocol differences are 52 axial slices with coverage of whole brain for standard DTI and 26 axial slices with coverage of fornix and cingulum plus an inversion time of 2,200 ms for FLAIR DTI (Concha et al., 2005b). Scan time for standard DTI and FLAIR DTI was 9:30 and 8:30 min, respectively. The signal to noise ratio (SNR) of the averaged b0 images in this study was high (approximately 66 for standard DTI and approximately 51 for FLAIR DTI).

Diffusion tensor tractography and region of interest analysis

Tensor calculation and tractography were performed on a PC running ExploreDTI (A. Leemans, University Medical Center, Utrecht, The Netherlands). The white matter tracts focused on the corpus callosum, limbic tracts, and connections to the frontal lobe. These structures were chosen based on previous observations in JME and IGE-GTC demonstrating: frontal lobe predominance of electroencephalographic changes (Montalenti et al., 2001); structural changes in frontal, parietal, and temporal lobe and cingulated cortex (Woermann et al., 1999; Betting et al., 2006a; Ciumas & Savic, 2006; Tae et al., 2006; Kim et al., 2007a; Tae et al., 2008; Bernhardt et al., 2009; O'Muircheartaigh et al., 2011) along with the corpus callosum (Tae et al., 2006; O'Muircheartaigh et al., 2011); and functional changes (executive function and memory), suggesting frontal lobe and limbic system dysfunction (Kim et al., 2007b). For practical reasons the tracts that were chosen are major white matter tracts that are well identified using deterministic tractography. Based on these, 12 major white matter tracts including the crus of fornix (Fx), dorsal cingulum (dCg), parahippocampal cingulum (pCg), genu/body/splenium of corpus callosum (gCC/bCC/sCC), inferior frontooccipital fasciculi (IFO), inferior/superior longitudinal fasciculi (ILF/SLF), uncinate fasciculi (UF), anterior limb of the internal capsule (ALIC), and corticospinal tracts (CST) were identified with tractography here (Fig. 1) and external capsule (EC), which cannot be reliably delineated with tractography, was analyzed with ROI. ExploreDTI, which adopts a deterministic streamline method to obtain fibers, was used to identify the Fx using the 26 slice FLAIR DTI data sets, whereas all the other tracts were delineated using the 52-slice standard DTI by setting the FA thresholds to 0.25 and the angular threshold to 60 degrees for UF and SLF and 30 degrees for all other tracts. ROIs were manually placed using a two ROI approach for each tract based on the methods and anatomy described before (Wakana et al., 2007; Malykhin et al., 2008). The bCC was defined as the central section of the corpus callosum excluding the genu, splenium, and tapetum. As a result, the bCC contains mainly fibers associated with premotor, supplementary motor, motor, and somatosensory cortices. FA was obtained by overlaying the tracts on FA maps and averaging all the voxels for both hemispheres to generate a single value per tract using an in-house program written by L.C. The external capsule (EC) was analyzed by manually drawing a ROI on a single axial FA map where the structure shows the clearest boundary.

Statistical analyses were administered using SPSS version 18 (SPSS Inc., Chicago, IL, U.S.A.). Paired Student's *t*-test was used to evaluate the right and left symmetry of 10

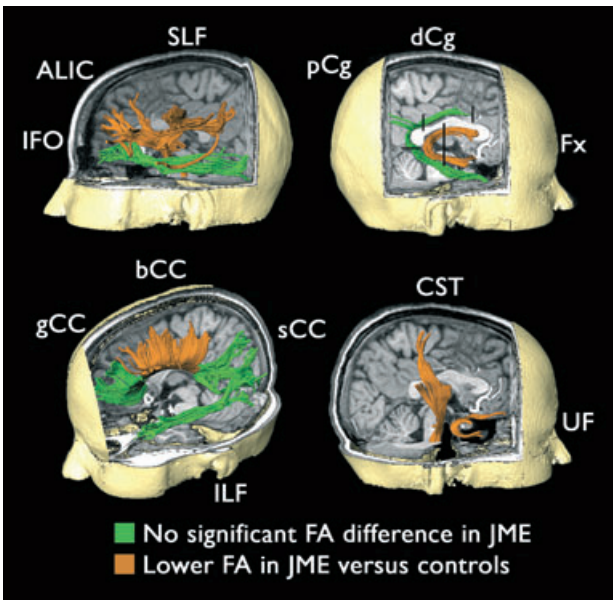

Figure 1.
Three-dimensional visualization of 12 tracts derived from tractography in a 17-year-old female JME patient. There was no statistically significant differences in FA between JME and controls for tracts in green, whereas tracts in orange had significantly lower FA in JME. Measurement of the fornix was constrained to the crus part as indicated by black lines cutting coronally at the fusion of left and right fornices. The dorsal cingulum was limited between the most posterior coronal slice of genu of corpus callosum and the most anterior coronal slice of splenium of the corpus callosum. The parahippocampal cingulum was limited below the lower body of the splenium. Fx, the crus of fornix; dCg, dorsal cingulum; pCg, parahippocampal cingulum; gCC/bCC/sCC, genu/body/splenium of corpus callosum; IFO, inferior frontooccipital fasciculi; ILF/SLF, inferior/superior longitudinal fasciculi; UF, uncinate fasciculi; ALIC, anterior limb of the internal capsule; and CST, corticospinal tracts.

paired tracts within JME patients, IGE-GTC patients, and each control group (the commissural tracts gCC/bCC/sCC are not included). The FA of Fx showed a small but significant asymmetry in JME patients (right = 0.42 ± 0.03; left = 0.43 ± 0.03; p = 0.03) and their corresponding 15 controls (right = 0.45 ± 0.02; left = 0.47 ± 0.02; p = 0.01), but not in IGE-GTC patients (right = 0.44 ± 0.03; left = 0.45 ± 0.02; p = 0.47) or their 10 matched controls (right = 0.46 ± 0.02; left = 0.45 ± 0.02; p = 0.6). The FA of SLF differed between left and right sides only in the 10 control group (right = 0.51 ± 0.02; left = 0.50 ± 0.02; p = 0.04) but not in the others. No asymmetry was observed for the other eight tracts. For simplicity, given the fact that most tracts were not asymmetric and those that were showed minimal FA differences, subsequent analysis was performed using collapsed data (i.e., a single mean value per subject combining both sides for each tract).

Before proceeding to the comparisons between patients and controls, the two control groups ($n_1 = 15$, $n_2 = 10$) were first tested against each other for FA of each of the 13 WM structures using an independent student *t*-test. The FA did not show a difference between the two control groups and the minimum p-value among the 13 tracts was 0.23. FA was then compared between the JME group (n = 15) and its corresponding control group (n = 15) and between the IGE-GTC group (n = 10) and its corresponding control group (n = 10) for each of the 13 WM structures using an independent *t*-test. Because the age and gender distributions were similar in the two comparisons, these variables were not included in the statistical model. False discovery rate (FDR) at p = 0.05 level was used to adjust for multiple comparison correction. To better understand the FA changes, parallel diffusivity ($\lambda_{||}$) and perpendicular diffusivity ($\lambda_{\perp}$), as well as mean diffusivity (MD), were queried subsequently for the tracts demonstrating significant between group differences using an independent student *t*-test. Furthermore, correlation between total lifetime GTC and FA of each abnormal tract within each patient group and in all patients combined was computed using Pearson's correlation coefficient at $p < 0.05$ with FDR correction.

Voxel-based morphometry on gray matter

Automated, whole-brain VBM was performed on T_1-weighted structural images using SPM8 (Wellcome Department of Cognitive Neurology, London, United Kingdom) and VBM8 toolbox (Revision 343, Christian Gaser, http://dbm.neuro.uni-jena.de/vbm/). In summary, all images were spatially normalized into the stereotaxic space using the high-dimensional Dartel method (Ashburner, 2007) and segmented into GM/WM/cerebrospinal fluid (CSF). The resultant GM images were modulated by Jacobian determinant only for the nonlinear terms so that not only the quantity of tissue that was deformed during nonlinear normalization was preserved but also individual brain sizes were corrected. This step yielded inference about regional GMV change in the following statistical analysis. The modulated GM images were smoothed using a 10-mm isotropic Gaussian Kernel. Relative GMV differences were assessed between the JME group (n = 15) and its corresponding control group (n = 15) and between the IGE-GTC group (n = 10) and its corresponding control group (n = 10) on a voxel wise basis using analysis of variance (ANOVA). An absolute GM threshold masking of 0.1 was applied to avoid confounding results around GM and WM edges and to exclude nonbrain voxels. Two T-contrast {1, −1} and {−1, 1} were defined for the comparisons to detect regional GMV increases or reductions. The voxel wise multiple comparisons were corrected using a FDR at $p < 0.05$ (Genovese et al., 2002). If no difference was found after FDR correction, a less stringent uncorrected threshold ($p < 0.001$) and

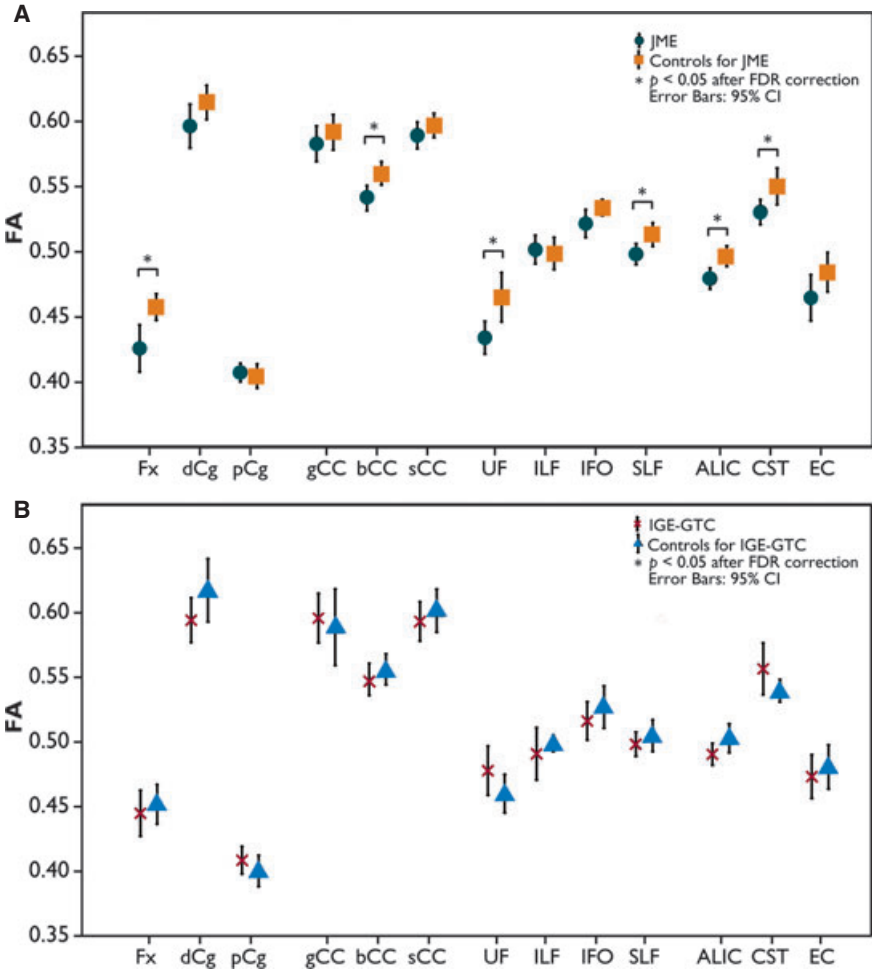

Figure 2.
Mean and 95% CI of fractional anisotropy (FA) for the 13 white matter structures (12 tracts analyzed with tractography as well as the external capsule, which was analyzed with ROIs) examined in JME with respect to its corresponding control group (panel **A**, n = 15 in each group) and in IGE-GTC with respect to its corresponding control group (panel **B**, n = 10 in each group). Significantly lower FA was observed in the six tracts marked by asterisks in JME, whereas no significant FA differences were detected in IGE-GTC. Fx, the crus of fornix; dCg, dorsal cingulum; pCg, parahippocampal cingulum; gCC/bCC/sCC, genu/body/splenium of corpus callosum; IFO, inferior frontooccipital fasciculi; ILF/SLF, inferior/superior longitudinal fasciculi; UF, uncinate fasciculi; ALIC, anterior limb of the internal capsule; and CST, corticospinal tracts.

extent threshold (k) defined by the expected number of voxels per cluster based on random field theory (readable from SPM output, k_{JME} = 106 voxels in the JME comparison and $k_{IGE\text{-}GTC}$ = 90 voxels in the IGE-GTC comparison) were used to detect potential GMV difference between groups. To probe a possible relationship between the identified GMV abnormality and total lifetime GTC, a correlation analysis was conducted by extracting the mean GMV within each abnormal cluster for each patient and correlating them with total lifetime GTC using Pearson's correlation coefficient at $p < 0.05$ with Bonferroni correction.

Results

Diffusion tensor tractography and region of interest analysis

No subjective differences of the 12 tracts between JME, IGE-GTC, and their corresponding controls was observed in terms of tract shape, and there were no differences in tract volume (data not shown, tested by independent *t*-test and $p < 0.05$). The FDR corrected *t*-tests demonstrated six tracts with significantly lower FA values in the JME group with respect to its control group, whereas there were no statistically significant differences between the IGE-GTC group and its corresponding control group (Figs. 1 and 2). The six tracts and their FDR corrected significance values as well as the percentages of FA reduction were as follows: Fx ($p = 0.036$, 6.9%), bCC ($p = 0.042$, 2.6%), UF ($p = 0.029$, 6.7%), SLF ($p = 0.043$, 2.9%), ALIC ($p = 0.019$, 3.5%), and CST ($p = 0.042$, 3.6%). The FA reduction resulted from an elevation of $\lambda_\perp$ in all cases ($p < 0.05$ in each individual tract without multiple comparison correction). There was no significant correlation between FA and lifetime GTC number in any of the six abnormal tracts for either JME group, IGE-GTC group, or in all epilepsy patients combined.

Voxel-based morphometry on gray matter

In regional gray matter volume (GMV), neither increases nor decreases were detected in JME or IGE-GTC patients as compared to their corresponding controls after FDR correction ($p < 0.05$). However, the spatial cluster extent corrected threshold showed GMV reduction in both JME and IGE-GTC, albeit in different regions (Fig. 3). JME patients showed GMV reductions in the right precentral gyrus (peak

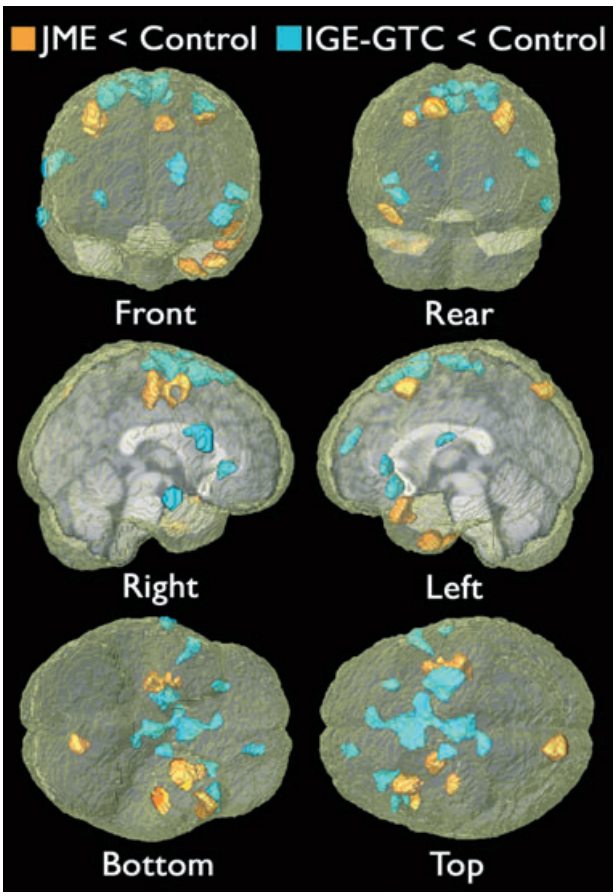

Figure 3.
VBM analyses detected regions that showed reduced gray matter volume (GMV) in JME (orange), IGE-GTC (blue) at a spatial cluster extent corrected statistical threshold ($p < 0.001$, $k_{JME} = 106$ voxels, $k_{IGE\text{-}GTC} = 90$ voxels) presented on the same 17-year-old female JME patient presented in Fig. 1 after the T_1-weighted image was transformed into Montreal Neurological Institute space. Regions of GMV reduction in JME included right precentral gyrus, left and right middle frontal gyri, left temporal pole, and left superior parietal gyrus. Regions of GMV reduction in IGE-GTC included left and right supplementary motor areas, left and right frontal lobes, left paracentral lobule, and right middle temporal gyrus. The detected regions in both patient groups were concentrated in frontal and central regions yet were separate from each other. JME GMV areas were more lateral and IGE-GTC GMV areas were more medial.

voxel, x, y, z = 33, −18, 49; T = 4.4), left and right middle frontal gyri (peak voxel, left x, y, z = −32, 15, 46, T = 4.53; right x, y, z = 35, 0, 51, T = 4.34), left temporal pole (peak voxel, x, y, z = −51, 18, −29, T = 3.86), and left superior parietal gyrus (peak voxel, x, y, z = −12, −76, 49, T = 4.02). The percentage reduction of these significant clusters in JME was19% compared to controls. IGE-GTC patients showed GMV reductions in left and right supplementary motor areas (peak voxel, left x, y, z = −5, 9, 70, T = 5.22; right x, y, z = 3, 8, 51; T = 4.95), left and right frontal lobes (peak voxel, left x, y, z = −44, 18, −12, T = 5.56; right x, y, z = 26, −7, 61; T = 5.16), left paracentral lobule (peak voxel, x, y, z = 0, −19, 67, T = 6.23), and right middle temporal gyrus (peak voxel, x, y, z = 69, −7, −17, T = 4.24). The percentage reduction of these significant clusters in IGE-GTC was 20% compared to controls. The detected regions in both patient groups were concentrated in frontal and central regions, but were separate from each other. JME GMV areas were more lateral, whereas IGE-GTC GMV areas were more medial. No significant correlation between the decreased GM region volumes of the significant clusters in JME and IGE-GTC patients and their total lifetime GTC number was observed at $p < 0.05$.

Discussion

The main finding of the study was that the two IGE subsyndromes, that is, JME and IGE-GTC, have distinct DTI findings, namely JME demonstrated reduction of FA in six white matter regions with four of them related to the temporal and/or frontal lobes, whereas IGE-GTC showed no such FA differences. Although corrected VBM analysis showed no differences between patient and control groups, the spatial extent cluster corrected VBM analysis suggested a trend of gray matter volume reduction in frontal and central regions in both patient groups, more lateral in JME and more medial in IGE-GTC.

Impaired white matter structures were demonstrated previously in JME patients based on a voxel-by-voxel comparison of FA maps (Deppe et al., 2008) and an ROI analysis in the frontal lobe and thalamocortical white matter (Keller et al., 2011). Our tractography findings of significant FA reductions in the anterior limb of the internal capsule (collapsed left and right) in JME are in agreement with the main finding of lowered FA in bilateral anterior limb of internal capsule (Deppe et al., 2008) and reduced FA in thalamocortical white matter fibers (Keller et al., 2011). Another DTI study of JME using probabilistic tractography demonstrated decreased FA in the connection of the supplementary motor area, which consists mainly of a portion of body of corpus callosum connecting to the contralateral supplementary motor area, and some ipsilateral corticospinal tracts (Vulliemoz et al., 2011). The same research group extended these findings on a larger JME sample by using TBSS to show FA reduction in the part of body of corpus callosum that projects to superior frontal regions, including the supplementary motor area (O'Muircheartaigh et al., 2011). Our finding of reduced FA in the body of corpus callosum is in agreement with these two studies. We also found reduced FA in the fornix, uncinate fasciculi, superior longitudinal fasciculi, and cortical spinal tracts in JME related to controls. It is interesting to note that the fornix, uncinate fasciculi, superior longitudinal fasciculi, and anterior limb of internal capsule were also reported abnormal in temporal

lobe epilepsy (McDonald et al., 2008; Ahmadi et al., 2009; Concha et al., 2009), suggesting the susceptibility of these white matter tracts in distinctly different epilepsy syndromes, whereas other affected tracts in temporal lobe epilepsy, such as inferior longitudinal fasciculi, inferior frontooccipital fasciculi and cingulum, were spared in JME. The percentage of FA reduction in the fornix observed in our JME patients (6.9%) was not as large as that of temporal lobe epilepsy patients with unilateral mesial temporal sclerosis (10%) previously reported by our group (Concha et al., 2005a, 2009). This could explain the mild or absent memory impairment reported in JME (O'Muircheartaigh et al., 2011) that is typically more severe in temporal lobe epilepsy (Oyegbile et al., 2004). On the other hand, the corticospinal tracts seem to be exclusively affected in JME but not in temporal lobe epilepsy (McDonald et al., 2008). The body of the corpus callosum, which connects bilateral motor regions, was abnormal in JME but not in temporal lobe epilepsy (Kim et al., 2008), whereas the genu and splenium were affected in temporal lobe epilepsy but not in JME (Deppe et al., 2008; O'Muircheartaigh et al., 2011; Vulliemoz et al., 2011). Using multiple analytic approaches such as VBA, TBSS, probabilistic tractography, and ROI analysis, the only DTI study on IGE-GTC showed reduced FA in cerebellum but not in the other white matter areas (Li et al., 2011). This is in agreement with the lack of DTI differences of IGE-GTC patients in our study. Because some of our DTI data did not cover the whole cerebellum due to the variation of individual brain size (cerebrums were fully covered primarily in these cases), we did not perform tractography for cerebellum tracts such as medial cerebellar peduncle.

The fact that the primary clinical difference between JME and IGE-GTC is the occurrence of myoclonus raises the possibility that disruption of white matter integrity may be the underlying mechanism responsible for myoclonus in JME. The reduced FA of the corticospinal tracts could be consistent with a disruption of the primary motor pathways in JME. Although it is impossible to confirm what underlying mechanism is responsible for the reduced FA observed in JME patients, an intriguing hypothesis would be that disruption of myelination is present, which in turn results in abnormal conduction of impulses in motor pathways resulting in ephaptic transmission as a possible explanation for the occurrence of myoclonus in JME.

The demonstration of ion channel and neurotransmitter receptor defects in Mendelian inherited IGE pedigrees has supported the assumption that changes in membrane excitability that occur at the molecular level are the primary pathophysiologic mechanism resulting in IGE (Cossette et al., 2002). Although previously considered to have no structural abnormalities, there is a growing body of quantitative imaging literature demonstrating such differences in IGE patients. Two reports on IGE patients with GTC as the predominant seizure type have demonstrated reduced GM (Ciumas & Savic, 2006; Bernhardt et al., 2009). The reported GM findings in JME have been more variable with some studies suggesting increased gray matter volume, whereas others reported decreased gray matter volume in different regions or no difference between JME and controls (Woermann et al., 1998, 1999; Ciumas & Savic, 2006; Tae et al., 2006; Roebling et al., 2009; O'Muircheartaigh et al., 2011). We did not find significant gray matter changes after multiple comparison correction, which is likely related to our relatively small sample size. Although caution must be maintained in drawing conclusions from VBM using spatial extent threshold due to the potential risk of false positives, the observation of reduced cortical gray matter volume bilaterally in both syndromes is in agreement with a number of previous studies (Ciumas & Savic, 2006; Tae et al., 2006; Bernhardt et al., 2009; O'Muircheartaigh et al., 2011). As opposed to previous reports (Ciumas & Savic, 2006; Kim et al., 2007a; Betting et al., 2010; Du et al., 2011), we did not observe volume difference of any subcortical gray matter in either patient group, which again may be explained by the relatively small sample size and the generality of the VBM method. A more dedicated volumetry study would be a better way to study subcortical gray matter specifically.

As previously stated, the current assumption is that sporadic JME and IGE-GTC are most likely caused by defects at the molecular level. Because it is difficult to directly associate an ion channel or neurotransmitter receptor defect with structural changes, the most reasonable explanation for the gray matter atrophy reported in both JME and IGE-GTC and the white matter abnormalities reported solely in JME by us and the other four previous studies is that these structural changes are a secondary effect of seizures (Deppe et al., 2008; Keller et al., 2011; O'Muircheartaigh et al., 2011; Vulliemoz et al., 2011). This concept was supported by the finding of Deppe et al. of a negative correlation between lifetime seizure number and FA. In contrast to their study, we did not find any correlations between lifetime seizures and FA for any white matter region, and we did not find any significant correlations between lifetime seizures and gray matter atrophy. Differences in subjects may account for this disagreement, in particular the fact that 3 of 10 subjects in the JME group of Deppe et al. had never experienced a generalized convulsion. Although the cross-sectional study design and relatively small number of subjects limit the conclusions that can be drawn from our study, our finding of an absence of a correlation does not support the idea that either the gray or white matter abnormalities are secondary to seizures. Because both the JME and IGE-GTC groups had experienced a similar number of lifetime generalized seizures (mean of 6, range 1–12 for JME and range 1–14 for IGE-GTC), the most compelling argument against the structural changes being secondary to seizures is that the two groups had distinctly different anatomic findings (different gray matter abnormalities in JME and IGE-GTC and white matter abnormalities in JME only), while

experiencing the same number of lifetime generalized tonic–clonic convulsions.

In summary, our findings demonstrate white matter abnormalities in JME but not in IGE-GTC and potential gray matter atrophy in both JME and IGE-GTC, which support the notion that JME and IGE-GTC may be associated with distinctly different anatomic substrates.

Acknowledgments

This work was supported by Canadian Institutes of Health Research (D.W.G. and C.B.); Alberta Innovates – Health Solutions (C.B.); and China Scholarship Council (M.L.). Thanks to Dr. Alexander Leemans for kindly providing DTI tractography analysis software and Dr. Catherine Lebel for technical advice.

Disclosure

None of the authors has any conflict of interest to disclose. We confirm that we have read the Journal's position on issues involved in ethical publication and affirm that this report is consistent with those guidelines.

References

Ahmadi ME, Hagler DJ Jr, McDonald CR, Tecoma ES, Iragui VJ, Dale AM, Halgren E. (2009) Side matters: diffusion tensor imaging tractography in left and right temporal lobe epilepsy. *AJNR Am J Neuroradiol* 30:1740–1747.

Andermann F, Berkovic SF. (2001) Idiopathic generalized epilepsy with generalized and other seizures in adolescence. *Epilepsia* 42:317–320.

Arfanakis K, Hermann BP, Rogers BP, Carew JD, Seidenberg M, Meyerand ME. (2002) Diffusion tensor MRI in temporal lobe epilepsy. *Magn Reson Imaging* 20:511–519.

Ashburner J. (2007) A fast diffeomorphic image registration algorithm. *Neuroimage* 38:95–113.

Basser PJ, Mattiello J, LeBihan D. (1994) MR diffusion tensor spectroscopy and imaging. *Biophys J* 66:259–267.

Beaulieu C. (2002) The basis of anisotropic water diffusion in the nervous system – a technical review. *NMR Biomed* 15:435–455.

Bernasconi A, Bernasconi N, Natsume J, Antel SB, Andermann F, Arnold DL. (2003) Magnetic resonance spectroscopy and imaging of the thalamus in idiopathic generalized epilepsy. *Brain* 126:2447–2454.

Bernhardt BC, Rozen DA, Worsley KJ, Evans AC, Bernasconi N, Bernasconi A. (2009) Thalamo-cortical network pathology in idiopathic generalized epilepsy: insights from MRI-based morphometric correlation analysis. *Neuroimage* 46:373–381.

Betting LE, Mory SB, Li LM, Lopes-Cendes I, Guerreiro MM, Guerreiro CA, Cendes F. (2006a) Voxel-based morphometry in patients with idiopathic generalized epilepsies. *Neuroimage* 32:498–502.

Betting LE, Mory SB, Lopes-Cendes I, Li LM, Guerreiro MM, Guerreiro CA, Cendes F. (2006b) MRI reveals structural abnormalities in patients with idiopathic generalized epilepsy. *Neurology* 67:848–852.

Betting LE, Li LM, Lopes-Cendes I, Guerreiro MM, Guerreiro CA, Cendes F. (2010) Correlation between quantitative EEG and MRI in idiopathic generalized epilepsy. *Hum Brain Mapp* 31:1327–1338.

Camfield P, Camfield C. (2010) Idiopathic generalized epilepsy with generalized tonic-clonic seizures (IGE-GTC): a population-based cohort with >20 year follow up for medical and social outcome. *Epilepsy Behav* 18:61–63.

Ciumas C, Savic I. (2006) Structural changes in patients with primary generalized tonic and clonic seizures. *Neurology* 67:683–686.

Concha L, Beaulieu C, Gross DW. (2005a) Bilateral limbic diffusion abnormalities in unilateral temporal lobe epilepsy. *Ann Neurol* 57:188–196.

Concha L, Gross DW, Beaulieu C. (2005b) Diffusion tensor tractography of the limbic system. *AJNR Am J Neuroradiol* 26:2267–2274.

Concha L, Beaulieu C, Collins DL, Gross DW. (2009) White-matter diffusion abnormalities in temporal-lobe epilepsy with and without mesial temporal sclerosis. *J Neurol Neurosurg Psychiatry* 80:312–319.

Concha L, Livy DJ, Beaulieu C, Wheatley BM, Gross DW. (2010) In vivo diffusion tensor imaging and histopathology of the fimbria-fornix in temporal lobe epilepsy. *J Neurosci* 30:996–1002.

Cossette P, Liu L, Brisebois K, Dong H, Lortie A, Vanasse M, Saint-Hilaire JM, Carmant L, Verner A, Lu WY, Wang YT, Rouleau GA. (2002) Mutation of GABRA1 in an autosomal dominant form of juvenile myoclonic epilepsy. *Nat Genet* 31:184–189.

Deppe M, Kellinghaus C, Duning T, Moddel G, Mohammadi S, Deppe K, Schiffbauer H, Kugel H, Keller SS, Ringelstein EB, Knecht S. (2008) Nerve fiber impairment of anterior thalamocortical circuitry in juvenile myoclonic epilepsy. *Neurology* 71:1981–1985.

Doelken MT, Mennecke A, Stadlbauer A, Kecskemeti L, Kasper BS, Struffert T, Doerfler A, Stefan H, Hammen T. (2010) Multi-voxel magnetic resonance spectroscopy at 3T in patients with idiopathic generalised epilepsy. *Seizure* 19:485–492.

Du H, Zhang Y, Xie B, Wu N, Wu G, Wang J, Jiang T, Feng H. (2011) Regional atrophy of the basal ganglia and thalamus in idiopathic generalized epilepsy. *J Magn Reson Imaging* 33:817–821.

Engel J Jr. (2001) A proposed diagnostic scheme for people with epileptic seizures and with epilepsy: report of the ILAE Task Force on Classification and Terminology. *Epilepsia* 42:796–803.

Genovese CR, Lazar NA, Nichols T. (2002) Thresholding of statistical maps in functional neuroimaging using the false discovery rate. *Neuroimage* 15:870–878.

Haki C, Gumustas OG, Bora I, Gumustas AU, Parlak M. (2007) Proton magnetic resonance spectroscopy study of bilateral thalamus in juvenile myoclonic epilepsy. *Seizure* 16:287–295.

Helms G, Ciumas C, Kyaga S, Savic I. (2006) Increased thalamus levels of glutamate and glutamine (Glx) in patients with idiopathic generalised epilepsy. *J Neurol Neurosurg Psychiatry* 77:489–494.

ILAE. (1989) Proposal for revised classification of epilepsies and epileptic syndromes. Commission on Classification and Terminology of the International League Against Epilepsy. *Epilepsia* 30:389–399.

Janz D. (1985) Epilepsy with impulsive petit mal (juvenile myoclonic epilepsy). *Acta Neurol Scand* 72:449–459.

Keller SS, Ahrens T, Mohammadi S, Moddel G, Kugel H, Bernd Ringelstein E, Deppe M. (2011) Microstructural and volumetric abnormalities of the putamen in juvenile myoclonic epilepsy. *Epilepsia* 52:1715–1724.

Kim JH, Lee JK, Koh S-B, Lee S-A, Lee J-M, Kim SI, Kang JK. (2007a) Regional grey matter abnormalities in juvenile myoclonic epilepsy: a voxel-based morphometry study. *Neuroimage* 37:1132–1137.

Kim SY, Hwang YH, Lee HW, Suh CK, Kwon SH, Park SP. (2007b) Cognitive impairment in juvenile myoclonic epilepsy. *J Clin Neurol* 3:86–92.

Kim H, Piao Z, Liu P, Bingaman W, Diehl B. (2008) Secondary white matter degeneration of the corpus callosum in patients with intractable temporal lobe epilepsy: a diffusion tensor imaging study. *Epilepsy Res* 81:136–142.

Koutroumanidis M, Smith S. (2005) Use and abuse of EEG in the diagnosis of idiopathic generalized epilepsies. *Epilepsia* 46:96–107.

Li Y, Du H, Xie B, Wu N, Wang J, Wu G, Feng H, Jiang T. (2011) Cerebellum abnormalities in idiopathic generalized epilepsy with generalized tonic-clonic seizures revealed by diffusion tensor imaging. *PLoS ONE* 5:e15219.

Lin K, Carrete H Jr, Lin J, Peruchi MM, de Araujo Filho GM, Guaranha MS, Guilhoto LM, Sakamoto AC, Yacubian EM. (2009) Magnetic resonance spectroscopy reveals an epileptic network in juvenile myoclonic epilepsy. *Epilepsia* 50:1191–1200.

Malykhin N, Concha L, Seres P, Beaulieu C, Coupland NJ. (2008) Diffusion tensor imaging tractography and reliability analysis for limbic and paralimbic white matter tracts. *Psychiatry Res* 164:132–142.

McDonald CR, Ahmadi ME, Hagler DJ, Tecoma ES, Iragui VJ, Gharapetian L, Dale AM, Halgren E. (2008) Diffusion tensor imaging correlates of memory and language impairments in temporal lobe epilepsy. *Neurology* 71:1869–1876.

Montalenti E, Imperiale D, Rovera A, Bergamasco B, Benna P. (2001) Clinical features, EEG findings and diagnostic pitfalls in juvenile myoclonic epilepsy: a series of 63 patients. *J Neurol Sci* 184:65–70.

Mory SB, Li LM, Guerreiro CA, Cendes F. (2003) Thalamic dysfunction in juvenile myoclonic epilepsy: a proton MRS study. *Epilepsia* 44:1402–1405.

Natsume J, Bernasconi N, Andermann F, Bernasconi A. (2003) MRI volumetry of the thalamus in temporal, extratemporal, and idiopathic generalized epilepsy. *Neurology* 60:1296–1300.

O'Muircheartaigh J, Vollmar C, Barker GJ, Kumari V, Symms MR, Thompson P, Duncan JS, Koepp MJ, Richardson MP. (2011) Focal structural changes and cognitive dysfunction in juvenile myoclonic epilepsy. *Neurology* 76:34–40.

Oyegbile TO, Dow C, Jones J, Bell B, Rutecki P, Sheth R, Seidenberg M, Hermann BP. (2004) The nature and course of neuropsychological morbidity in chronic temporal lobe epilepsy. *Neurology* 62:1736–1742.

Roebling R, Scheerer N, Uttner I, Gruber O, Kraft E, Lerche H. (2009) Evaluation of cognition, structural, and functional MRI in juvenile myoclonic epilepsy. *Epilepsia* 50:2456–2465.

Savic I, Lekvall A, Greitz D, Helms G. (2000) MR spectroscopy shows reduced frontal lobe concentrations of *N*-acetyl aspartate in patients with juvenile myoclonic epilepsy. *Epilepsia* 41:290–296.

Savic I, Osterman Y, Helms G. (2004) MRS shows syndrome differentiated metabolite changes in human-generalized epilepsies. *Neuroimage* 21:163–172.

Seeck M, Dreifuss S, Lantz G, Jallon P, Foletti G, Despland PA, Delavelle J, Lazeyras F. (2005) Subcortical nuclei volumetry in idiopathic generalized epilepsy. *Epilepsia* 46:1642–1645.

Tae W, Hong S, Joo E, Han S, Cho J, Seo D, Lee J, Kim I, Byun H, Kim S. (2006) Structural brain abnormalities in juvenile myoclonic epilepsy patients: volumetry and voxel-based morphometry. *Korean J Radiol* 7:162–172.

Tae WS, Kim SH, Joo EY, Han SJ, Kim IY, Kim SI, Lee JM, Hong SB. (2008) Cortical thickness abnormality in juvenile myoclonic epilepsy. *J Neurol* 255:561–566.

Thivard L, Lehericy S, Krainik A, Adam C, Dormont D, Chiras J, Baulac M, Dupont S. (2005) Diffusion tensor imaging in medial temporal lobe epilepsy with hippocampal sclerosis. *Neuroimage* 28:682–690.

Vulliemoz S, Vollmar C, Koepp MJ, Yogarajah M, O'Muircheartaigh J, Carmichael DW, Stretton J, Richardson MP, Symms MR, Duncan JS. (2011) Connectivity of the supplementary motor area in juvenile myoclonic epilepsy and frontal lobe epilepsy. *Epilepsia* 52:507–514.

Wakana S, Caprihan A, Panzenboeck MM, Fallon JH, Perry M, Gollub RL, Hua K, Zhang J, Jiang H, Dubey P, Blitz A, van Zijl P, Mori S. (2007) Reproducibility of quantitative tractography methods applied to cerebral white matter. *Neuroimage* 36:630–644.

Woermann FG, Sisodiya SM, Free SL, Duncan JS. (1998) Quantitative MRI in patients with idiopathic generalized epilepsy. Evidence of widespread cerebral structural changes. *Brain* 121(Pt 9):1661–1667.

Woermann F, Free S, Koepp M, Sisodiya S, Duncan J. (1999) Abnormal cerebral structure in juvenile myoclonic epilepsy demonstrated with voxel-based analysis of MRI. *Brain* 122(Pt 11):2101–2108.

Yogarajah M, Focke NK, Bonelli S, Cercignani M, Acheson J, Parker GJ, Alexander DC, McEvoy AW, Symms MR, Koepp MJ, Duncan JS. (2009) Defining Meyer's loop-temporal lobe resections, visual field deficits and diffusion tensor tractography. *Brain* 132:1656–1668.

Zifkin B, Andermann E, Andermann F. (2005) Mechanisms, genetics, and pathogenesis of juvenile myoclonic epilepsy. *Curr Opin Neurol* 18:147–153.